NATIONAL ADVISORY COMMITTEE FOR AERONAUTICS

TECHNICAL NOTE 4022

ESTIMATION OF COMPRESSIBLE BOUNDARY-LAYER GROWTH OVER INSULATED SURFACES WITH PRESSURE GRADIENT

By Gerald W. Englert

Lewis Flight Propulsion Laboratory
Cleveland, Ohio

Washington

June 1957

NATIONAL ADVISORY COMMITTEE FOR AERONAUTICS

TECHNICAL NOTE 4022

ESTIMATION OF COMPRESSIBLE BOUNDARY-LAYER GROWTH OVER INSULATED SURFACES WITH PRESSURE GRADIENT

By Gerald W. Englert

SUMMARY

The incompressible boundary-layer theory of Truckenbrodt was extended using a modified Stewartson-type transformation to include compressible boundary-layer development over insulated surfaces. The variation of turbulent shear stresses with Mach number of the bounding potential stream was considered using the reference-temperature method of Eckert. The explicit technique of Truckenbrodt for determining the profile parameter in the incompressible theory was unchanged so that the profile parameter as well as the momentum thickness can still be evaluated by simple quadratures in the present theory.

The method is applicable to two-dimensional and axisymmetric, laminar and turbulent boundary layer, and accounts for the pressure gradient along the wall for both compressible and incompressible flow.

Experimental measurements of the boundary layer on small axisymmetric bodies on the wall of a supersonic wind tunnel were compared with theoretical predictions. For most cases studied, agreement between experiment and theory was within 10 percent.

INTRODUCTION

It was first shown by von Kármán (ref. 1) that the differential equations describing the motion of the fluid in a boundary layer can be simplified by use of integral thickness parameters. The resulting integral equations then consider the growth of these parameters (momentum and displacement thicknesses) in the external stream direction. References 2 and 3 further showed that for incompressible flow all velocity profiles could be reasonably represented by one parameter family; this profile parameter generally being the ratio of displacement to momentum thickness. Determination of any two of these three parameters, momentum thickness, displacement thickness, and profile parameter, therefore, is sufficient to describe the over-all boundary-layer profile characteristics for most engineering applications.

The momentum equation has been solved by the Kármán-Pohlhausen-Holstein method (ref. 2, pp. 93-100) for the laminar incompressible case. A method of calculation of the plane turbulent boundary layer was first made by Gruschwitz (ref. 4, pp. 93-98). Von Doenhoff and Tetervin (ref. 3) also presented a method for calculation of two-dimensional turbulent boundary layer, the procedure of which was later simplified by Garner (ref. 5). Explicit expressions for momentum thickness in terms of a simple quadrature were obtained by Buri (ref. 6) and Maskell (ref. 7) for plane turbulent flow, and by Walz (ref. 8) for plane laminar flow.

Recent progress has been made by Truckenbrodt (ref. 9) who devised a method for computing laminar and turbulent boundary layer for both two-dimensional and axisymmetric flow. The main advantage of this method over references 2 to 8 is that it enables the computation of the profile parameter as well as the momentum thickness in explicit form by use of simple quadratures.

References 2 to 9 all consider incompressible boundary layer. Stewartson (ref. 10) presented relations which transformed the two-dimensional, compressible laminar boundary-layer equation to the form of the incompressible case. Cohen and Reshotko (refs. 11 and 12) applied these transformations to the laminar boundary layer including the effects of heat transfer. Van Le (ref. 13) suggested that the Stewartson-type transformation be used for turbulent as well as laminar flow if time average values were taken for the variables. Reshotko and Tucker (ref. 14) and Mager (ref. 15) used these transformations for analysis of shock-induced turbulent boundary-layer separation.

This paper uses a modified Stewartson transformation to change the final equations of Truckenbrodt to compressible coordinates for both two-dimensional and axisymmetric flow. The results should then be applicable to laminar or turbulent, two-dimensional or axisymmetric, compressible or incompressible adiabatic flows with or without surface pressure gradients. The explicit form developed by Truckenbrodt for evaluating boundary-layer profile parameter and momentum thickness by means of simple quadratures is retained.

SYMBOLS

A	friction term defined by eq. (5)
a	sonic velocity
b	constant in eq. (10)
C	constant in eq. (2)

c_f	local coefficient of friction
$c_{f,av}$	average coefficient of friction
d	dissipation (energy converted into heat)
H	profile parameter δ^*/θ
$\overline{H}$	profile parameter δ^{**}/θ
K	parameter used in eq. (9)
L	profile parameter (fig. 1)
l	total length of boundary layer in longitudinal direction
M	local Mach number
n	constant = 1 for laminar flow, 1/6 for turbulent flow
p	pressure
R	transformed body radius
r	body radius
T	temperature
t	turbulence energy
U	longitudinal velocity component at edge of boundary layer, $y = \delta$
u	longitudinal velocity component
X	transformed longitudinal coordinate
x	longitudinal coordinate
Y	transformed normal coordinate
y	normal coordinate
α	constant in eq. (10)
γ	ratio of specific heats
δ	boundary-layer height

δ^*	displacement thickness
δ^{**}	energy thickness
ε	variable in eq. (24)
ζ	defined by eq. (23)
θ	momentum thickness
$\varkappa$	defined by eq. (22)
μ	absolute viscosity
ν	kinematic viscosity
ξ	defined by eq. (12)
ρ	density
τ	shear stress (includes both laminar and time average turbulent stresses if any)
φ	cone half angle

Subscripts:

e	edge of boundary layer, $y = \delta$
I	incompressible flow in "physical" space
i	transformed or incompressible flow
l	laminar
0	free-stream stagnation conditions
p	flat plate
r	recovery
s	starting, or initial, conditions
T	transition
t	turbulent
w	wall or surface value

Superscript:

* based on Eckert's reference temperature used everywhere except when modifying δ

THEORY

Incompressible Momentum Thickness

A brief review, to aid in the understanding of the final expressions used from reference 9, will be given.

The Truckenbrodt method of computing momentum thickness is based on Wieghardt's kinetic energy equation,

$$\frac{1}{U_i^3 R}\frac{d}{dX}\left(U_i^3 R \bar{H}_i \theta_i\right) = 2\frac{d+t}{\rho_0 U_i^3} = 2\int_0^{\delta_i}\frac{\tau_w}{\rho_0 U_i^2}\frac{\partial \frac{u_i}{U_i}}{\partial Y}\,dY \qquad (1)$$

instead of the momentum integral equation used by references 2 to 8. Use of the energy equation offers the advantage that the term representing the sum of the dissipation and turbulence energies $(d + t/\rho_0 U_i^3)$ is almost independent of profile parameter H_i, whereas the friction coefficient, which enters into the momentum equation, varies rapidly with profile parameter. The dissipation term was studied as a function of H_i and $U_i\theta_i/\nu_0$ by use of Hartree profiles for laminar flow and the results of references 16 and 17 for turbulent flow.

Equation (1) was therefore integrated, assuming mean values for H_i, resulting in

$$\theta_i\left(\frac{U_i\theta_i}{\nu_0}\right)^n = \frac{C + A\int_{X_s}^{X} U_i^{3+2n} R^{1+n}\,dX}{U_i^{3+2n} R^{1+n}} \qquad (2)$$

where the integration constant $C = U_{i,s}^{3+2n} R_s^{1+n}\left(\frac{U_{i,s}\theta_{i,s}}{\nu_0}\right)^n \theta_{i,s}$

The subscript s denotes initial conditions. The constant n equals 1 for laminar flow and 1/6 for turbulent flow.

The coefficient A was evaluated by Truckenbrodt by assuming that the average shearing stress at the wall was of the same form as that for

a flat plate at zero incidence. For a flat plate U_i is constant and $\theta_{i,s} = 0$ if $X_s = 0$, so that equation (2) becomes

$$\left(\frac{\theta_{i,p}U_{i,p}}{\nu_0}\right)^n \theta_{p,i} = Al_i$$

and since for a flat plate from the momentum integral equation

$$\frac{\theta}{l} = \frac{c_{f,av}}{2}$$

$$A = \left(\frac{U_i l_i}{\nu_0}\right)^n \left(\frac{c_{f,i,av}}{2}\right)^{1+n} \tag{3}$$

The average wall friction coefficient was in turn evaluated for laminar flow by the Blasius equation

$$c_{f_l,i_{av}} = \frac{1.328}{\sqrt{\frac{U_i l_i}{\nu_0}}} \tag{4}$$

and for turbulent flow by the Falkner expression

$$c_{f_t,i_{av}} = \frac{0.0306}{\left(\frac{U_i l_i}{\nu_0}\right)^{1/7}} \tag{5}$$

so that

$A = 0.441$ for laminar flow

$A = 0.0076$ for turbulent flow

The two-dimensional case is obtained by omitting R in equations (1) and (2). It is interesting to note that the formula for momentum thickness (eq. (2)) has the same form as that given by Buri (ref. 6) and Maskell (ref. 7) for turbulent flow, and by Walz (ref. 8) for laminar flow, in spite of widely different methods of derivation. The exponent on $U_i\theta_i/\nu_0$ is given as 0.25, 0.2155, and 0.167 for turbulent flow by references 6, 7, and 9, respectively, whereas the exponent on the U_i term is given as 4.0, 4.2, and 3.33, and the A constants are 0.015, 0.01173, and 0.0076. For laminar flow, $n = 1$ in both references 8 and 9. Reference 8 lists A as 0.470 in place of the 0.441 value in reference 9.

When considering both laminar and turbulent flow, the final expression by Truckenbrodt for momentum thickness may be written as

$$\theta_i = \frac{1}{U_i^3 R}\left\{\left[A_l \nu_0 \int_0^{X_T} U_i^5 R^2 \, dX\right]^{7/12} + A_t \nu_0^{1/6} \int_{X_T}^{X} U_i^{10/3} R^{7/6} \, dX\right\}^{6/7} \tag{6}$$

where X_T is the longitudinal distance to transition. The expression inside the brackets is the contribution of the laminar boundary layer, and the remaining part inside the braces is the contribution of the turbulent boundary layer.

Incompressible Profile Parameter

As stated in the INTRODUCTION, the method of reference 9 for determining the profile parameter differs from the other methods in that Truckenbrodt succeeded in determining the profile parameter in an explicit form. The momentum equation

$$\frac{1}{U_i^2 R} \frac{d}{dX}(U_i^2 R \theta_i) + H_i \frac{\theta_i}{U_i} \frac{dU_i}{dX} = \frac{\tau_{w,i}}{\rho_0 U_i^2} \tag{7}$$

was subtracted from the kinetic energy equation (1) making

$$\theta_i \frac{d\bar{H}_i}{dX} = (H_i - 1)\bar{H}_i \frac{\theta_i}{U_i} \frac{dU_i}{dX} + 2 \frac{d + t}{\rho_0 U_i^3} - \bar{H}_i \frac{\tau_{w,i}}{\rho_0 U_i^2} \tag{8}$$

Note that this expression is independent of R. Equation (8) was rearranged to the following form:

$$\left(\frac{U_i \theta_i}{\nu_0}\right)^n \theta_i \frac{dL}{dX} = \left(\frac{U_i \theta_i}{\nu_0}\right)^n \frac{\theta_i}{U_i} \frac{dU_i}{dX} - K(L_i) \tag{9}$$

where the profile parameter L_i is defined by

$$L_i = \int_{\bar{H}_{p,i}}^{\bar{H}_i} \frac{d\bar{H}_i}{(H_i - 1)\bar{H}_i}$$

and

$$K(L) = \frac{-\left(2 \frac{d + t}{\rho_0 U_i^2} - \bar{H}_i \frac{\tau_{w,i}}{\rho_0 U_i^2}\right)\left(\frac{U_i \theta_i}{\nu_0}\right)^n}{(H_i - 1)\bar{H}_i}$$

The quantity L_i was arbitrarily chosen as zero for zero pressure gradient flows so that the value of $H_{p,i}$ was set at 2.6 for laminar flow and at 1.4 for turbulent flow.

The data of references 16 to 19 for turbulent flow, and the Hartree profiles (numerically evaluated in ref. 20) for laminar flow were used to arrive at approximate expressions for K as a function of L_i, and L_i as a function of H_i.

An adequate approximation for the quantity $K(L_i)$ is

$$K(L_i) = \alpha(L_i - b) \tag{10}$$

where

$$\alpha = \begin{cases} 2.87 \text{ for laminar flow with pressure drop} \\ 3.53 \text{ for laminar flow with pressure rise} \\ 0.0304 \text{ for turbulent flow} \end{cases}$$

$$b = \begin{cases} 0 \text{ for laminar flow} \\ 0.0305 \ln U_i\theta_i/\nu_0 - 0.23 \text{ for turbulent flow} \end{cases}$$

The resulting relations between L_i and H_i are shown in figure 1.

Substitution of equation (10) in equation (9) results in a first degree linear differential equation, then solved for L_i. The result is

$$L_i = \frac{\xi_{s,i}}{\xi_i} L_{s,i} + \ln\left(\frac{U_i}{U_{s,i}}\right) + \frac{1}{\xi_i} \int_{\xi_{s,i}}^{\xi_i} \left[b - \ln\left(\frac{U_i}{U_{s,i}}\right)\right] d\xi_i \tag{11}$$

where

$$\xi_{i,l} = \left[A_l \nu_0 \int_0^{X_T} U_i^5 R^2 \, dX\right]^{(\alpha/A)_l} \tag{12a}$$

for laminar flow

$$\xi_{i,t} = \left\{\left[A_l \nu_0 \int_0^{X_T} U_i^5 R^2 \, dX\right]^{7/12} + A_t \nu_0^{1/6} \int_{X_T}^{X} U_i^{10/3} R^{7/16} \, dX\right\}^{(\alpha/A)_t} \tag{12b}$$

for turbulent flow. The parameter ξ_i is defined by the two equations (12a) and (12b) since the change of profile parameter through the transition region will be handled as a discontinuity, as will be discussed later in the Initial Conditions section.

The calculation procedure may be briefly summarized as follows: for a given velocity distribution over a known body, the momentum thickness distribution is first calculated using equation (6); then the profile parameter L_i is calculated as a function of the longitudinal distance from equations (11) and (12), and finally, the conventional form factor H_i is obtained from the values of L_i using figure 1.

Transformation to Compressible Case

A modified Stewartson transformation for a Prandtl number of one and an adiabatic flow (see Appendix and symbol list) is

$$\left.\begin{aligned} X &= \int_0^x \left(\frac{a_e}{a_0}\right)^{\frac{3\gamma-1}{\gamma-1}} dx \\ Y &= \frac{a_e}{a_0}\int_0^y \frac{\rho}{\rho_0}\, dy \\ U_i &= a_0 M_e = \frac{a_0}{a_e} U \\ u_i &= \frac{a_0}{a_e} u \\ R &= r \end{aligned}\right\} \tag{A1}$$

Where x, y, and r are the compressible "physical" coordinates and X, Y, and R are the transformed coordinates. Use of these transformations in either the Kármán momentum equation or the Wieghardt kinetic energy equation yields the following relation for the friction coefficient (see Appendix).

$$c_{f,i} \equiv \frac{\tau_{i,w}}{\frac{1}{2}\rho_0 U_i^2} = \left(\frac{a_0}{a_e}\right)^2 c_f \equiv \left(\frac{a_0}{a_e}\right)^2 \frac{\tau_w}{\frac{1}{2}\rho_e U^2} \tag{13}$$

For laminar flow

$$c_{f_{i,l}} = \frac{\mu_0\left(\frac{\partial u_i}{\partial Y}\right)_{Y=0}}{\frac{1}{2}\rho_0 U_i^2} = \frac{\mu_0\left[\frac{\partial\left(\frac{a_0}{a_e}u\right)}{\partial y}\frac{a_0}{a_e}\frac{\rho_0}{\rho_e}\left(\frac{a_0}{a_e}\right)^2\right]_{y=0}}{\frac{1}{2}\rho_e U^2\left(\frac{a_0}{a_e}\right)^2\frac{\rho_0}{\rho_e}} = c_{f,l}\left(\frac{a_0}{a_e}\right)^2 \quad (14)$$

Therefore the transformations satisfy the known relations for the laminar friction coefficient.

For turbulent flow, the total shear term includes turbulent as well as laminar shear stresses, and no simple expression for the total stresses is available. Eckert (ref. 21), however, found that the form of the expression for a flat plate friction coefficient can be made invariant with the Mach number of the external stream when the properties of the fluid are based on a proper reference temperature. This reference temperature is described as

$$T^* = T_e + 0.5(T_w - T_e) + 0.22(T_r - T_e)$$

or

$$\frac{T^*}{T_e} = 0.72\frac{T_w}{T_e} + 0.28$$

if

$$T_w = T_r$$

Expressions for friction coefficient obtained for incompressible flows can then be extended to apply to compressible flows. From reference 21

$$c_f = \frac{\tau}{\frac{1}{2}\rho_e U^2} = \frac{\rho^*}{\rho_e}c_f^* \quad (15)$$

Applying this method to equation (4) of this report and assuming that the viscosity varies linearly with temperature,

$$\frac{\mu}{\mu_0} = \frac{T}{T_0} = \left(\frac{a}{a_0}\right)^2$$

The effect of compressibility on the turbulent friction coefficient could be shown through the ratio

$$\frac{c_{f_t}}{c_{f_{I,t}}} = \frac{\left(\frac{\rho_e U l}{\mu_e}\right)^{1/7}}{\left(\frac{\rho^* U l}{\mu^*}\right)^{1/7}} \frac{\rho^*}{\rho_e} = \left(\frac{a_e}{a^*}\right)^{10/7} \tag{16}$$

where c_{f_I} is defined as the constant fluid-property (incompressible) friction coefficient for the same Reynolds number as the compressible stream and should be kept distinct from the incompressible friction coefficient c_{f_i} in the transformed plane. The agreement between the results of equation (16)($\gamma = 1.4$) and those of references 21 to 26 is shown in figure 2. The curve of equation (16) is somewhat lower than that of reference 21, based upon the Schultz-Grunow equation (ref. 27). Closer agreement of equation (16) with reference 21 and the experimental data could have been obtained by adjustment of the constants in the expression for reference temperature. This adjustment was not believed necessary for purposes of the present study.

A transformation of the compressible friction coefficient by use of equations (A1), (5), and (15) results in

$$c_{f_t} = c^*_{f_t} \frac{\rho^*}{\rho_e} = \frac{0.0306}{\left(\frac{\rho^* U l}{\mu^*}\right)^{1/7}} \frac{\rho^*}{\rho_e}$$

$$= \frac{0.0306\left(\frac{a_e}{a^*}\right)^2}{\left[\left(\frac{a_e}{a^*}\right)^2\left(\frac{a_e}{a_0}\right)^{\frac{2}{\gamma-1}} \rho_0 \frac{a_e}{a_0} U_i \left(\frac{a_0}{a_e}\right)^{\frac{3\gamma-1}{\gamma-1}} l_i \left(\frac{a_0}{a^*}\right)^2 \frac{1}{\mu_0}\right]^{1/7}}$$

$$= \left(\frac{a_e}{a_0}\right)^{4/7}\left(\frac{a_e}{a^*}\right)^{10/7} \frac{0.0306}{\left(\frac{\rho_0 U_i l_i}{\mu_0}\right)^{1/7}} \tag{17}$$

In figure 3 it is shown that

$$\frac{a_e}{a^*} = \left(\frac{a_e}{a_0}\right)^{6/7} \tag{18}$$

so that equation (17) becomes

$$c_{f_t} = \left(\frac{a_e}{a_0}\right)^{88/49} \frac{0.0306}{\left(\frac{\rho_0 U_i l}{\mu_0}\right)^{1/7}}$$

Therefore, the transformed friction coefficient may be expressed as

$$c_{f_{i,t}} = \left(\frac{a_0}{a_e}\right)^2 c_{f_t}$$

$$= \frac{0.0306}{\left(\frac{\rho_0 U_i l}{\mu_0}\right)^{1/7}} \left(\frac{a_0}{a_e}\right)^{10/49} \tag{19}$$

Recall that friction coefficient enters into equation (6) through the A terms, where for turbulent flow

$$A_t = \left(\frac{U_i l_i}{\nu_0}\right)^{1/6} \left(\frac{c_{f_i}}{2}\right)^{7/6}$$

A combination of this equation with equation (19) yields

$$A_t = 0.0076 \left(\frac{a_0}{a_e}\right)^{5/21} \tag{20}$$

When $M_e \to 0$, $\frac{a_0}{a_e} \to 1$ so that equation (6) remains unaltered for incompressible flow.

Therefore, under the circumstances considered (insulated surface and Prandtl number equals one) the laminar boundary layer is exactly transformed to the incompressible form, whereas the turbulent boundary layer is transformed to a form which reduces to the incompressible form for a Mach number of zero.

A transformation of equation (6) by means of equations (A1) and (20) to get the compressible flow momentum thickness gives

$$\theta = \frac{1}{\left(\frac{a_e}{a_0}\right)^{\frac{\gamma+1}{\gamma-1}} M_e^3 r} \left\{ \left[\frac{0.441\nu_0}{a_0} \int_0^{x_T} M_e^5 r^2 \left(\frac{a_e}{a_0}\right)^{\frac{3\gamma-1}{\gamma-1}} dx \right]^{7/12} + \frac{0.0076 \left(\frac{\nu_0}{a_0}\right)^{1/6}}{\left(\frac{a_e}{a_0}\right)^{5/21}} \int_{x_T}^{x} M_e^{10/3} r^{7/6} \left(\frac{a_e}{a_0}\right)^{\frac{3\gamma-1}{\gamma-1}} dx \right\}^{6/7} = \frac{\varkappa^{6/7}}{\left(\frac{a_e}{a_0}\right)^{\frac{\gamma+1}{\gamma-1}} M_e^3 r} \tag{21}$$

where

$$\varkappa = \zeta^{7/12} + \frac{0.0076 \left(\frac{\nu_0}{a_0}\right)^{1/6}}{\left(\frac{a_e}{a_0}\right)^{5/21}} \int_{x_T}^{x} M_e^{10/3} r^{7/6} \left(\frac{a_e}{a_0}\right)^{\frac{3\gamma-1}{\gamma-1}} dx \tag{22}$$

and

$$\zeta = \frac{0.441\nu_0}{a_0} \int_0^{x_T} M_e^5 r^2 \left(\frac{a_e}{a_0}\right)^{\frac{3\gamma-1}{\gamma-1}} dx \tag{23}$$

For the completely laminar boundary-layer case, $\varkappa$ equals $\zeta^{7/12}$, and for the completely turbulent case, $\varkappa$ equals only the second term on the right side of equation (22).

When determining the profile parameter, it is convenient first to determine L_i and then find H_i and H. By substituting equations (A1) and (20) in expressions (11) and (12), and by using the definitions of a and b, the following equation results:

$$L_i = \left(\frac{\varepsilon_s}{\varepsilon}\right) L_{i,s} + \ln\left(\frac{M_e}{M_{e,s}}\right) + \frac{1}{\varepsilon} \int_{\varepsilon_s}^{\varepsilon} \left[b - \ln\left(\frac{M_e}{M_{e,s}}\right) \right] d\varepsilon \tag{24}$$

where

$\varepsilon = \zeta^{6.5}$ for laminar flow with pressure drop

$\varepsilon = \zeta^{8}$ for laminar flow with pressure rise

$\varepsilon = \kappa^{4\left(\frac{a_e}{a_0}\right)^{5/21}}$ for turbulent flow

$b = 0$ for laminar flow

$$b = 0.0305 \ln\left[\left(\frac{a_e}{a_0}\right)^{\frac{2}{\gamma-1}} \frac{U\theta}{\nu_0}\right] - 0.23 \quad \text{for turbulent flow}$$

Figure 1 can now be used to determine H_i. A combination of equations (A3) and (A5) results in the following expression for H:

$$H = \left(\frac{a_0}{a_e}\right)^2 (H_i + 1) - 1 \tag{25}$$

Boundary-layer profile and momentum thickness for compressible flow can thus be determined in explicit form by use of equations (21) to (25). Recall that these equations are written in the more general or axisymmetric case. For two-dimensional flow merely omit r whenever it appears.

Initial Conditions

Initial values for laminar flow are derived in reference 9 as follows: For two-dimensional stagnation-point flow,

$$L_{i,s} = 0.0260$$

$$\theta_{i,s} = \frac{0.271}{\sqrt{\frac{1}{\nu_0}\frac{dU_i}{dX}}}$$

or

$$\theta_s = \frac{0.271}{\sqrt{\frac{1}{\nu_0}\frac{dU}{dx}\left(\frac{a_e}{a_0}\right)^{\frac{9\gamma-13}{2\gamma-2}}}}$$

For axisymmetric stagnation-point flow,

$$L_{i,s} = 0.0195$$

$$\theta_{i,s} = \frac{0.235}{\sqrt{\frac{1}{\nu_0}\frac{dU_i}{dX}}}$$

or

$$\theta_s = \frac{0.235}{\sqrt{\frac{1}{\nu_0}\frac{dU}{dx}}}\left(\frac{a_e}{a_0}\right)^{\frac{9\gamma-13}{2\gamma-2}}$$

For both two-dimensional and axisymmetric flow over a sharp-edged or pointed body,

$$L_{i,s} = 0$$

and (26)

$$\theta_{i,s} = \theta_s = 0$$

There will be a relatively small change in θ through the transition region if the length of the boundary-layer travel is large, therefore, it is reasonable to assume that θ_t at the end of the transition is equal to θ_l at the start of transition. Appreciable change in the profile parameter, however, may take place through the transition region. For incompressible flow with no pressure gradient, reference 9 lists the measured results of references 27, 16, and 17 as shown in figure 4. These results show only a small variation of change of the incompressible profile parameter through transition as a function of the Reynolds number. Some data for transition showing a large effect of the pressure gradient may be found in reference 7 for incompressible flow. Inaccurate assumptions of the initial value of H are quite permissible, however, because the influence of the values selected for an initial condition vanishes rapidly with the distance downstream of the transition. This will be demonstrated later in the EXPERIMENT section.

EXPERIMENT

The method advanced in this report was compared with a limited amount of experimental measurements of the boundary layer on several small axisymmetric bodies and on the walls of a large supersonic tunnel.

The measurements were made with small pitot tubes. Momentum thickness and form factors were computed with the assumption that static pressure and total temperature were constant in the y-direction through the boundary layer. These assumptions are the same as those of the appendix. The Reynolds number (Ul/ν) was approximately 5×10^6 for the axisymmetric bodies and approximately 2×10^9 for the supersonic tunnel. The transition Reynolds number was approximately 1.5×10^6 on the axisymmetric bodies. The boundary layer on the tunnel was essentially completely turbulent.

Comparison of theory with measurement made on cones having half angles of 20° and 25° is shown in figure 5. For the case of the constant pressure gradient ($dp/dx = 0$), equations (21) can be integrated to give

$$\theta = \frac{1}{\left(\frac{a_e}{a_0}\right)^{\frac{\gamma+1}{\gamma-1}} M_e^3 r} \left\{ \left[\frac{0.147\nu_0 \sin^2\varphi\, M_e^5 \left(\frac{a_e}{a_0}\right)^{\frac{3\gamma-1}{\gamma-1}} x_T^3}{a_0} \right]^{7/12} + 0.00351 \left(\frac{\nu_0}{a_0}\right)^{1/6} M_e^{10/3} \sin^{7/6}\varphi \left(\frac{a_e}{a_0}\right)^{\frac{58\gamma-16}{21\gamma-21}} \left(x^{13/6} - x_T^{13/6}\right) \right\}^{6/7}$$

Thus, no integrals need be evaluated to determine the momentum thickness. The largest difference between experimental and theoretical momentum thickness is 7 percent, which is probably close to experimental accuracy.

The change of the profile parameter (H or H_i) with the turbulent boundary-layer growth is negligibly small on these cones since there is no pressure gradient in the x-direction and the length of the boundary-layer development is approximately 1 foot. These data therefore were used as a check of the profile-parameter transformation (eq. (25)). The compressible profile parameter was computed from the incompressible profile-parameter values of 1.3 and 1.4. This is the maximum range of H_i obtained using equation (26) and figure 4. Good agreement with the experimental trend was obtained.

Figures 6 and 7 compare theoretical and experimental results for the cases of moderate and high, adverse pressure gradient ($dp/dx > 0$). The abrupt pressure gradient on figure 7 is due to an externally generated shock striking the body. These bodies are all conical for $0 \leqq x \leqq 0.233$, in which range it was assumed that $dp/dx = 0$. The experimental Mach number variation with distance in the x-direction is

shown in figures 6(a) and 7(a), and the calculated momentum and displacement variation is shown in figures 6(b) and 7(b). The agreement is generally within 10 percent, which is again close to the accuracy of the data.

The effect of making an erroneous assumption of the initial value of the profile parameter is also shown in figure 6(b) by the line made up of short dashes. An initial value of 2.2 (near separation value) was assigned to H_i even though the pressure gradient in this region was small. In spite of this poor assumption, the solution converged to the original curve (in which H_i was assumed to be 1.4) in a very short distance.

The case of a favorable pressure gradient ($dp/dx < 0$) on the wall of a supersonic tunnel is shown in figure 8. Since the flow in this case was neither completely axisymmetric or two-dimensional, an effective radius equal to the tunnel wetted perimeter at each axial station and divided by 2π was used for r in equation (21). This computed result was compared with the experimental θ and H measured on two adjacent tunnel walls. Experimental agreement with theory was generally within 10 percent.

Only small changes in the incompressible profile parameter (H_i) were obtained in the cases of the favorable and moderate adverse pressure gradient. Large changes, however, were obtained for the compressible profile parameter (H). Therefore, for rough approximations in these cases and when initial conditions are known quite well, it may be permissible to hold H_i constant and determine H from equation (25) only, thus eliminating the use of equation (24). Obviously, the elimination of equation (24) would not be permissible for boundary layers in the region of large adverse pressure gradients.

CONCLUDING REMARKS

A method has been presented herein which enables a determination of the compressible boundary-layer growth and profile over both two-dimensional and axisymmetric bodies. Both momentum thickness and profile parameter are obtained by simple quadratures. The method includes both laminar and turbulent flow; however, the experimental check involved mainly turbulent flow. The momentum thickness at the transition point was calculated to be approximately 10 percent of the total momentum thickness for the cones and axisymmetric bodies. Comparison was made between theory and experiment for flows with zero, adverse, and favorable pressure gradients in the direction of boundary-layer travel. For most cases studied, agreement between experiment and theory was within 10 percent.

Lewis Flight Propulsion Laboratory
National Advisory Committee for Aeronautics
Cleveland, Ohio, April 16, 1957

APPENDIX - TRANSFORMATION OF MOMENTUM AND ENERGY EQUATIONS

The modified Stewartson transformation used in this report is:

$$\left.\begin{aligned} X &= \int_0^x \left(\frac{a_e}{a_0}\right)^{\frac{3\gamma-1}{\gamma-1}} dx \\ Y &= \frac{a_e}{a_0}\int_0^y \frac{\rho}{\rho_0}\, dy \\ U_i &= a_0 M_e = \frac{a_0}{a_e} U \\ u_i &= \frac{a_0}{a_e} u \end{aligned}\right\} \quad (A1)$$

and for axisymmetric flow it will be shown that the radius is invariant with these transformations so that

$$R = r$$

These relations will be used to transform the compressible momentum and energy equations to corresponding equations of the incompressible form. In like manner, it could be shown that these relations can be used for the inverse transformations, that is, from the incompressible to the compressible form.

It will be assumed that there is no heat transfer, that the Prandtl number equals one, that static pressure is constant in the y-direction for $0 \leqslant y \leqslant \delta$, and that the flow external to the boundary layer is isentropic.

Any of the equations in this appendix can be applied to two-dimensional flow by omitting the r and R terms.

Momentum Equation

The Kármán momentum integral equation for axisymmetric compressible flow can be written as follows:

$$\frac{1}{r\rho_e U^2}\frac{d}{dx}(r\rho_e U^2\theta) + \frac{1}{U}\frac{dU}{dx}\delta^* = \frac{\tau_w}{\rho_e U^2} \quad (A2)$$

To transform this equation, some useful relations will be derived. By definition

$$\theta = \int_0^{\delta} \frac{\rho u}{\rho_e U}\left(1 - \frac{u}{U}\right)dy$$

and by using equation (A1)

$$\theta = \frac{a_0\rho_0}{a_e\rho_e}\int_0^{\delta_i} \frac{u_i}{U_i}\left(1 - \frac{u_i}{U_i}\right)dY$$

then also

$$\theta = \left(\frac{a_0}{a_e}\right)^{\frac{\gamma+1}{\gamma-1}} \theta_i \tag{A3}$$

By definition

$$\delta^* = \int_0^{\delta} \left(1 - \frac{\rho u}{\rho_e U}\right)dy$$

with equation (A1)

$$\delta^* = \frac{a_0}{a_e}\frac{\rho_0}{\rho_e}\int_0^{\delta_i}\left[1 + \frac{\gamma - 1}{2} M_e^2\left(1 - \frac{u_i^2}{U_i^2}\right) - \frac{u_i}{U_i}\right]dY$$

since

$$\frac{\rho_e}{\rho} = \frac{T}{T_e} = 1 + \frac{\gamma - 1}{2} M_e^2\left(1 - \frac{u_i^2}{U_i^2}\right) \tag{A4}$$

therefore,

$$\delta^* = \left(\frac{a_0}{a_e}\right)^{\frac{\gamma+1}{\gamma-1}}\int_0^{\delta_i}\left[1 - \frac{u_i}{U_i} + \frac{\gamma - 1}{2} M_e^2\left(1 - \frac{u_i}{U_i} + \frac{u_i}{U_i} - \frac{u_i^2}{U_i^2}\right)\right]dY$$

$$= \left(\frac{a_0}{a_e}\right)^{\frac{\gamma+1}{\gamma-1}}\left[\delta_i^* + \frac{\gamma - 1}{2} M_e^2\left(\delta_i^* + \theta_i\right)\right] \tag{A5}$$

From equation (A1)

$$\frac{dU_i}{dX} = \left(\frac{a_0}{a_e}\right)^{\frac{4\gamma-2}{\gamma-1}} \frac{dU}{dx} + U \frac{d\left(\frac{a_0}{a_e}\right)}{dx}\left(\frac{a_0}{a_e}\right)^{\frac{3\gamma-1}{\gamma-1}}$$

and

$$\frac{d\left(\frac{a_0}{a_e}\right)}{dx} = \frac{\gamma - 1}{2}\left(\frac{a_0}{a_e}\right)\frac{M_e^2}{U}\frac{dU}{dx}$$

since

$$\frac{a_0}{a_e} = \left(\frac{\rho_0}{\rho_e}\right)^{\frac{\gamma-1}{2}} \tag{A6}$$

and

$$dp_e = -\rho_e U\, dU \tag{A7}$$

Therefore,

$$\frac{dU}{dx} = \frac{\left(\frac{a_e}{a_0}\right)^{\frac{4\gamma-2}{\gamma-1}} \frac{dU_i}{dX}}{1 + \frac{\gamma - 1}{2} M_e^2} \tag{A8}$$

and

$$\frac{d\left(\frac{a_e}{a_0}\right)}{dX} = \frac{-\frac{\gamma - 1}{2}\frac{M_e^2}{U_i}\frac{a_e}{a_0}\frac{dU_i}{dX}}{1 + \frac{\gamma - 1}{2} M_e^2} \tag{A9}$$

By substituting equations (A1), (A3), (A5), (A6), and (A8) in equation (A2)

$$\frac{\frac{a_e}{a_0}}{U_i^2 R}\frac{d}{dX}\left[\left(\frac{a_e}{a_0}\right)U_i^2 R\theta_i\right] +$$

$$\frac{1}{U_i}\frac{dU_i}{dX}\frac{\left(\frac{a_e}{a_0}\right)^2}{1 + \frac{\gamma - 1}{2} M_e^2}\left[\delta_i^* + \frac{\gamma - 1}{2}\left(M_e^2\,\delta_i^* + \theta_i\right)\right] = \frac{\tau_w}{\rho_e U^2}$$

After using equation (A9) and collecting terms, there results

$$\frac{1}{U_i^2 R}\frac{d}{dX}(U_i^2 R\theta_i) + \frac{\delta_i^*}{U_i}\frac{dU_i}{dX} = \left(\frac{a_0}{a_e}\right)^2 \frac{\tau_w}{\rho_e U^2} \tag{A10}$$

and thus the momentum equation takes the incompressible form if $(a_0/a_e)^2\,\tau_w/\rho_e U^2 = \tau_{i,w}/\rho_0 U_i^2$. This transformation of the friction term is discussed in the THEORY section of this report.

4326

Energy Equation

The kinetic energy integral equation of Wieghardt for axisymmetric compressible flow may be written in the following integral form:

$$\frac{1}{2\rho_e U^3 r}\frac{d}{dx}(\rho_e U^3 r\delta^{**}) - \frac{1}{U}\frac{dU}{dx}\int_0^\delta \frac{u}{U}\left(\frac{\rho}{\rho_e} - 1\right)dy = \int_0^\delta \frac{\tau_w}{\rho_e U^2}\frac{\partial \frac{u}{U}}{\partial y}\,dy \tag{A11}$$

Equations (A1), (A6), and (A8) are substituted in equation (A11) to give:

$$\frac{1}{2U_i^3 R}\frac{d}{dX}\left[\left(\frac{a_e}{a_0}\right)^2 U_i^3 R\delta_i^{**}\right] -$$

$$\frac{\frac{1}{U_i}\left(\frac{a_e}{a_0}\right)^{\frac{3\gamma-1}{\gamma-1}}\frac{dU_i}{dX}}{1 + \frac{\gamma-1}{2}M_e^2}\int_0^{\delta_i} \frac{u_i}{U_i}\frac{\rho_0 a_0}{\rho_e a_e}\left(1 - \frac{\rho_e}{\rho}\right)dY = \int_0^\delta \frac{\tau}{\rho_e U^2}\frac{\partial \frac{u_i}{U_i}}{\partial Y}\,dY \tag{A12}$$

since

$$\delta^{**} = \int_0^\delta \frac{\rho u}{\rho_e U}\left(1 - \frac{u^2}{U^2}\right)dy = \frac{\rho_0 a_0}{\rho_e a_e}\int_0^\delta \frac{u_i}{U_i}\left(1 - \frac{u_i^2}{U_i^2}\right)dY$$

$$= \frac{\rho_0 a_0}{\rho_e a_e}\,\delta_i^{**}$$

By using equations (A4) and (A9) in equation (A12),

$$\frac{1}{2U_i^3R}\frac{d}{dX}(U_i^3R\delta_i^{**}) - \frac{\frac{\gamma-1}{2}\frac{M_e^2}{U_i}\frac{dU_i}{dX}}{1+\frac{\gamma-1}{2}M_e^2}\int_0^{\delta_i}\frac{u_i}{U_i}\left(1-\frac{u_i^2}{U_i^2}\right)dY +$$

$$\frac{\frac{1}{U_i}\frac{dU_i}{dX}}{1+\frac{\gamma-1}{2}M_e^2}\int_0^{\delta_i}\frac{u_i}{U_i}\frac{\gamma-1}{2}M_e^2\left(1-\frac{u_i^2}{U_i^2}\right)dY = \int_0^{\delta_i}\left(\frac{a_0}{a_e}\right)^2\frac{\tau_w}{\rho_e U^2}\frac{\partial\frac{u_i}{U_i}}{\partial y_i}\,dY$$

and by collecting terms,

$$\frac{1}{2U_i^3R}\frac{d}{dX}(U_i^3R\delta_i^{**}) = \int_0^{\delta_i}\left(\frac{a_0}{a_e}\right)^2\frac{\tau_w}{\rho_e U^2}\frac{\partial\frac{u_i}{U_i}}{\partial Y}\,dY \qquad (A13)$$

which is the incompressible form of the Wieghardt kinetic energy equation if $(a_0/a_e)^2\,\tau_w/\rho_e U^2 = \tau_{i,w}/\rho_0 U_i^2$. Thus, if the friction transformation is satisfied in the momentum equation, it is satisfied in the Wieghardt kinetic energy equation.

4526

REFERENCES

1. von Kármán, Th.: Über laminare und turbulente Reibung. Z.a.M.M., Bd. 1, Heft 4, Aug. 1921, pp. 233-252.

2. Schlichting, H.: Lecture Series "Boundary Layer Theory." I - Laminar Flows. NACA TM 1217, 1949.

3. von Doenhoff, Albert E., and Tetervin, Neal: Determination of General Relations for the Behavior of Turbulent Boundary Layers. NACA Rep. 772, 1943. (Supersedes NACA WRL-382.)

4. Schlichting, H.: Lecture Series "Boundary Layer Theory." II - Turbulent Flows. NACA TM 1218, 1949.

5. Garner, H. C.: The Development of Turbulent Boundary Layers. R. and M. No. 2133, British ARC, June 1944.

6. Goldstein, S., ed.: Modern Developments in Fluid Dynamics. Vol. II. Clarendon Press (Oxford), 1938, p. 436.

7. Maskell, E. C.: Approximate Calculation of the Turbulent Boundary Layer in Two-Dimensional Incompressible Flow. Rep. No. AERO 2443, British RAE, Nov. 1951.

8. Walz, A.: Ein neuer Ansatz fur das Geschwindigkeitsprofile der laminaren Reibungschicht. Lilienthal-Bericht, Bd. 141, 1941, p. 8.

9. Truckenbrodt, E.: A Method of Quadrature for Calculation of the Laminar and Turbulent Boundary Layer in Case of Plane and Rotationally Symmetrical Flow. NACA TM 1379, 1955.

10. Stewartson, K.: Correlated Incompressible and Compressible Boundary Layers. Proc. Roy. Soc. (London), ser. A, vol. 200, no. A1060, Dec. 22, 1949, pp. 84-100.

11. Cohen, Clarence B., and Reshotko, Eli: Similar Solutions for the Compressible Laminar Boundary Layer with Heat Transfer and Pressure Gradient. NACA Rep. 1293, 1956. (Supersedes NACA TN 3325.)

12. Cohen, Clarence B., and Reshotko, Eli: The Compressible Laminar Boundary Layer with Heat Transfer and Arbitrary Pressure Gradient. NACA Rep. 1294, 1956. (Supersedes NACA TN 3326.)

13. Van Le, Nguyen: Transformation Between Compressible and Incompressible Boundary-Layer Equations. Jour. Aero. Sci., vol. 20, no. 8, Aug. 1953, pp. 583-584.

14. Reshotko, Eli, and Tucker, Maurice: Effect of a Discontinuity on Turbulent Boundary-Layer-Thickness Parameters with Application to Shock Induced Separation. NACA TN 3454, 1955.

15. Mager, Artur: Prediction of Shock-Induced Turbulent Boundary-Layer Separation. Jour. Aero. Sci., vol. 22, no. 3, Mar. 1955, pp. 201-202.

16. Rotta, J. (E. N. Labouvie, trans.): Contribution to the Calculation of Turbulent Boundary Layers. Trans. 242, Navy Dept., The David W. Taylor Model Basin, Nov. 1951.

17. Rotta, J.: Schubspannungs verteilung und Energiedissipation bei turbulenten Grenzschichten. Inc.-Arch., Bd. XX, Heft 3, 1952, pp. 195-207.

18. Wieghardt, K., and Tillmann, W.: On the Turbulent Friction Layer for Rising Pressure. NACA TM 1314, 1951.

19. Ludwieg, H., and Tillmann, W.: Investigations of the Wall-Shearing Stress in Turbulent Boundary Layers. NACA TM 1285, 1950.

20. Walz, A.: Anwendung des Energiestazes von Wieghardt auf einparametrige Geschwindigkeitsprofile in laminaren Grenzschichten. Ing.-Arch., Bd. XVI, 1948, pp. 243-248.

21. Eckert, E. R. G.: Engineering Relation for Friction and Heat Transfer to Surfaces in High Velocity Flow. Jour. Aero. Sci., vol. 22, no. 8, Aug. 1955, pp. 585-586.

22. Wilson, Robert E.: Turbulent Boundary-Layer Characteristics at Supersonic Speeds - Theory and Experiment. Jour. Aero. Sci., vol. 17, no. 9, Sept. 1950, pp. 585-594.

23. Chapman, Dean R., and Kester, Robert H.: Turbulent Boundary-Layer and Skin-Friction Measurements in Axial Flow Along Cylinders at Mach Numbers Between 0.5 and 3.6. NACA TN 3097, 1954.

24. Coles, D.: Measurements in the Boundary Layer on a Smooth Flat Plate in Supersonic Flow. Ph.D. Thesis, C.I.T., 1953.

25. Lobb, R. Kenneth, Winkler, Eva M., and Persh, Jerome: Experimental Investigation of Turbulent Boundary Layer in Hypersonic Flow. Jour. Aero. Sci., vol. 22, no. 1, Jan. 1955, pp. 1-9; 50.

26. von Kármán, Th.: The Problem of Resistance in Compressible Fluids. Reale Accademia d'Italia (Rome), T. XIII, 1935.

27. Schultz-Grunow, F.: New Frictional Resistance Law for Smooth Plates. NACA TM 986, 1941.

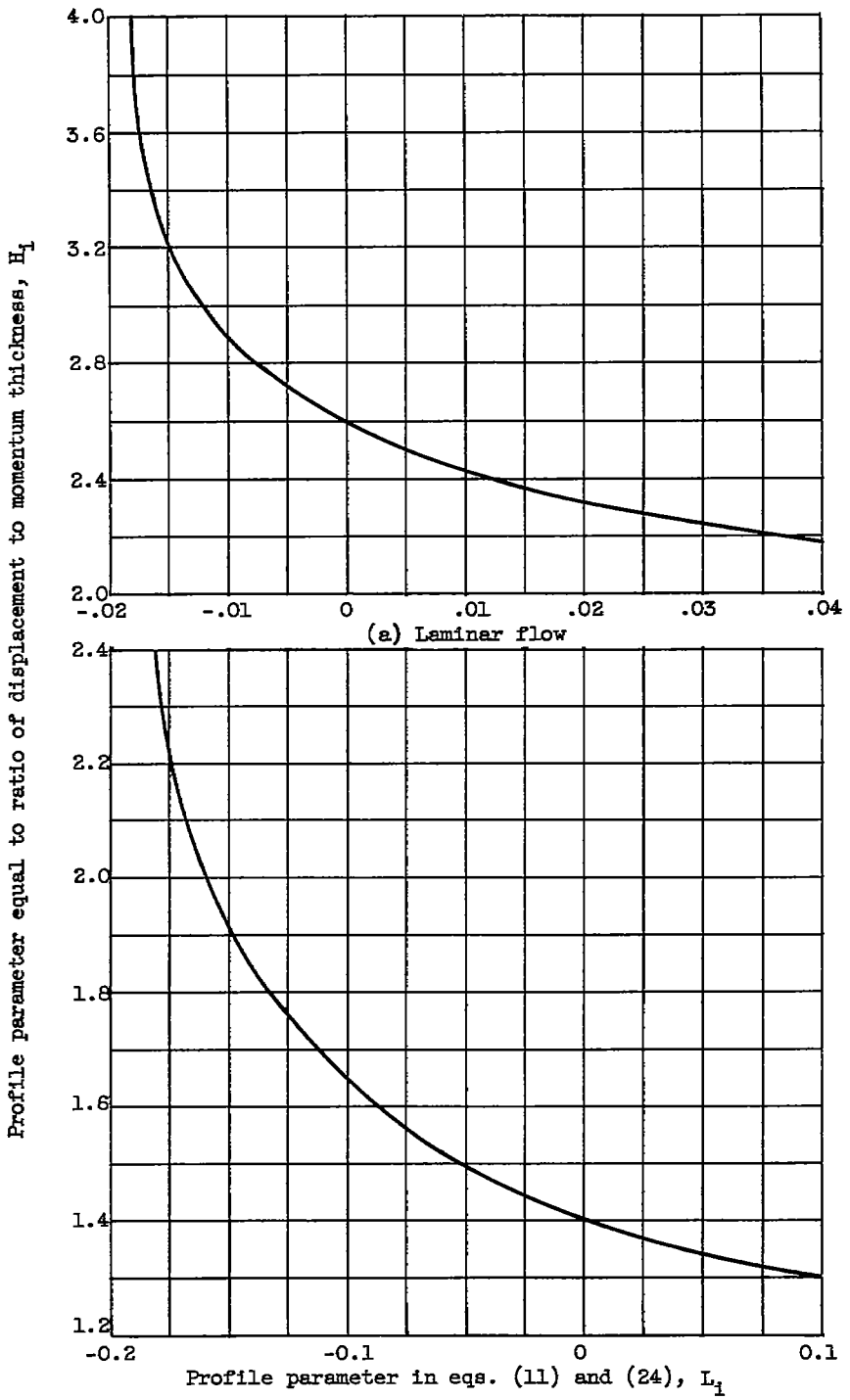

Figure 1. - Relations between incompressible boundary-layer profile parameters (ref. 9).

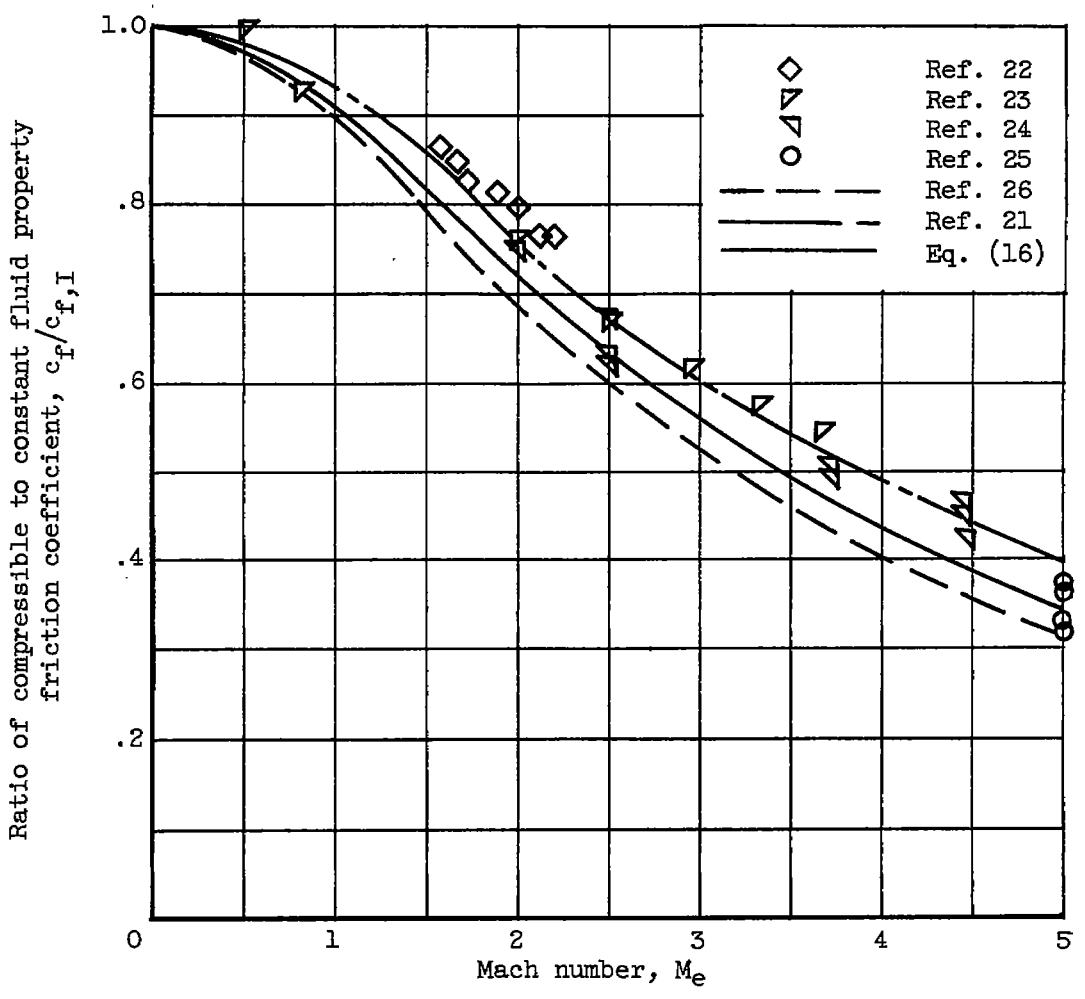

Figure 2. - Effect of compressibility on skin friction of a flat plate.

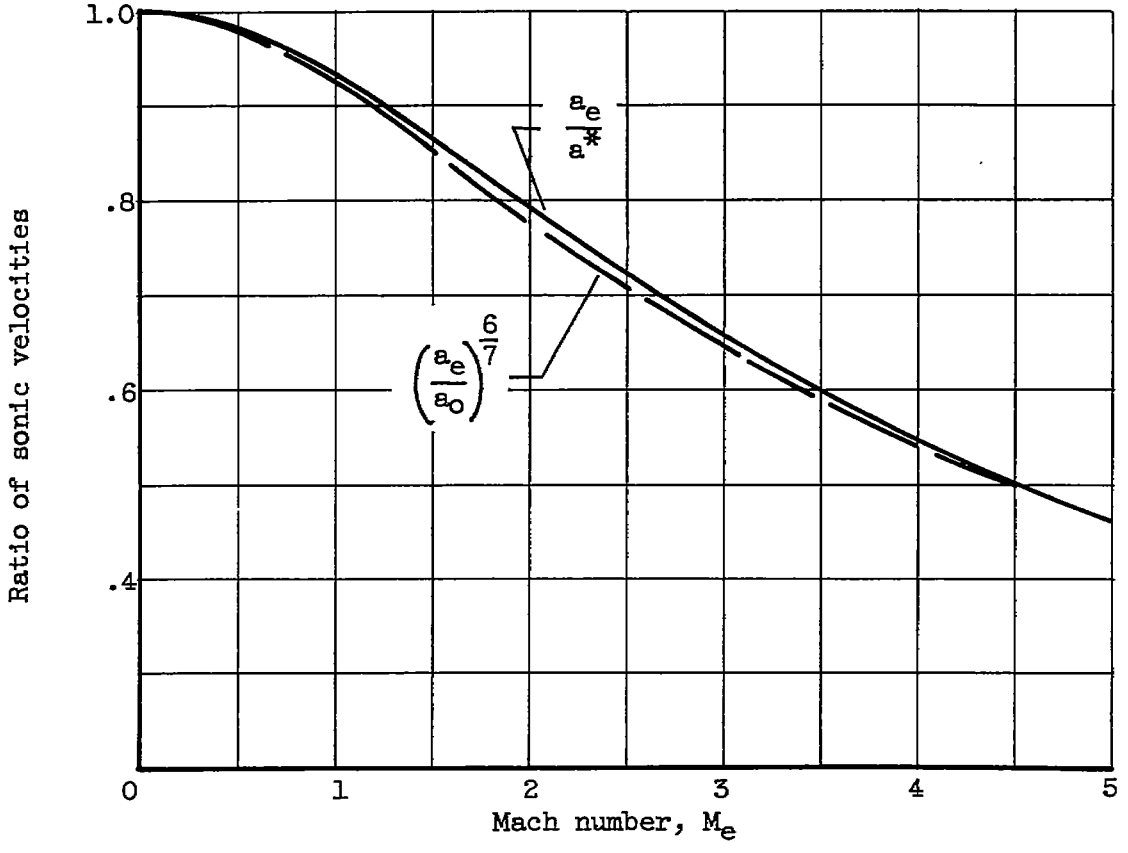

Figure 3. - Comparison of speed of sound based on reference temperature of Eckert with speed of sound based on stagnation temperature. Ratio of specific heat, 1.4.

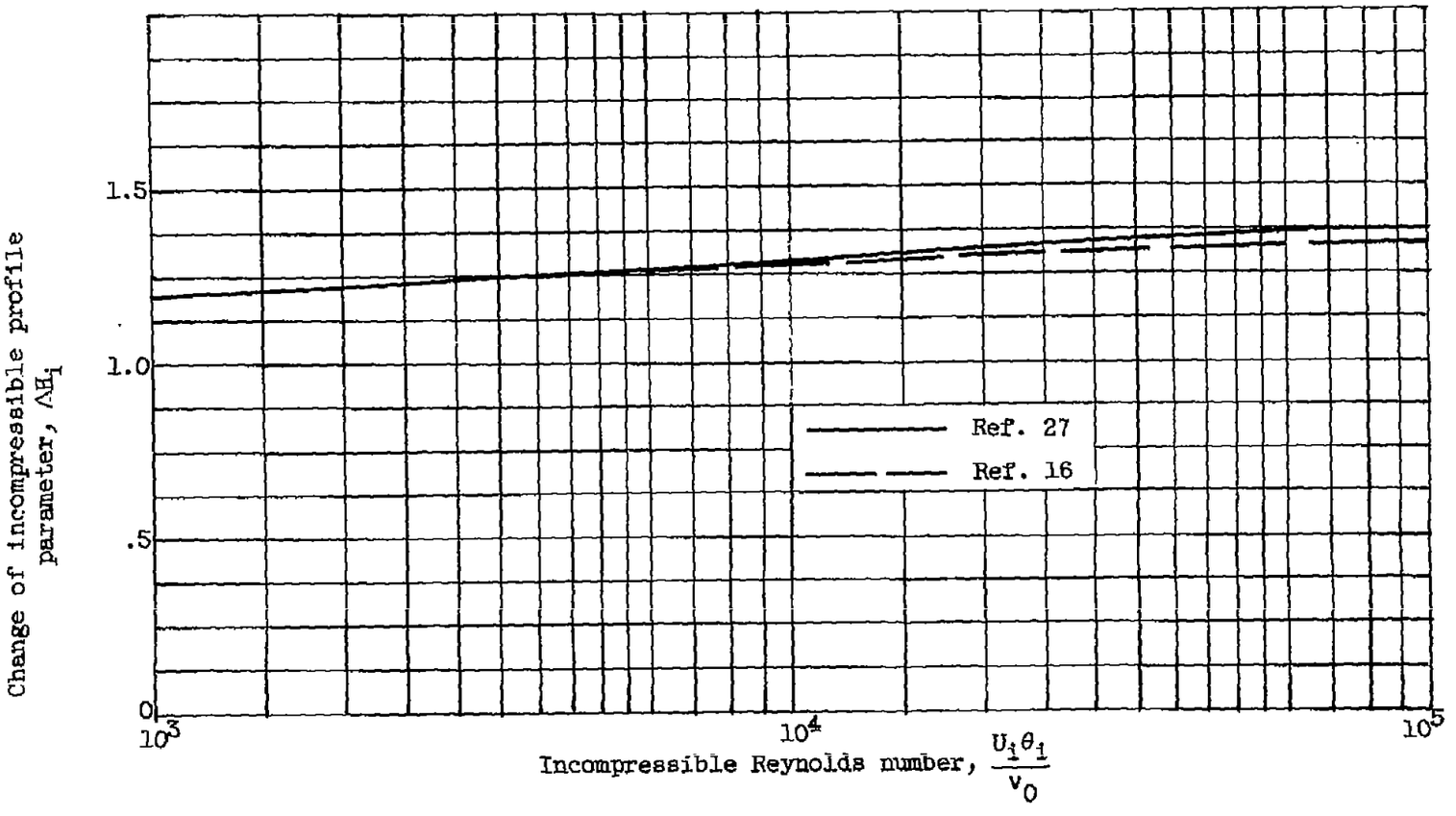

Figure 4. - Change of incompressible form factor in the range of transition from laminar to turbulent flow (ref. 9). No pressure gradient.

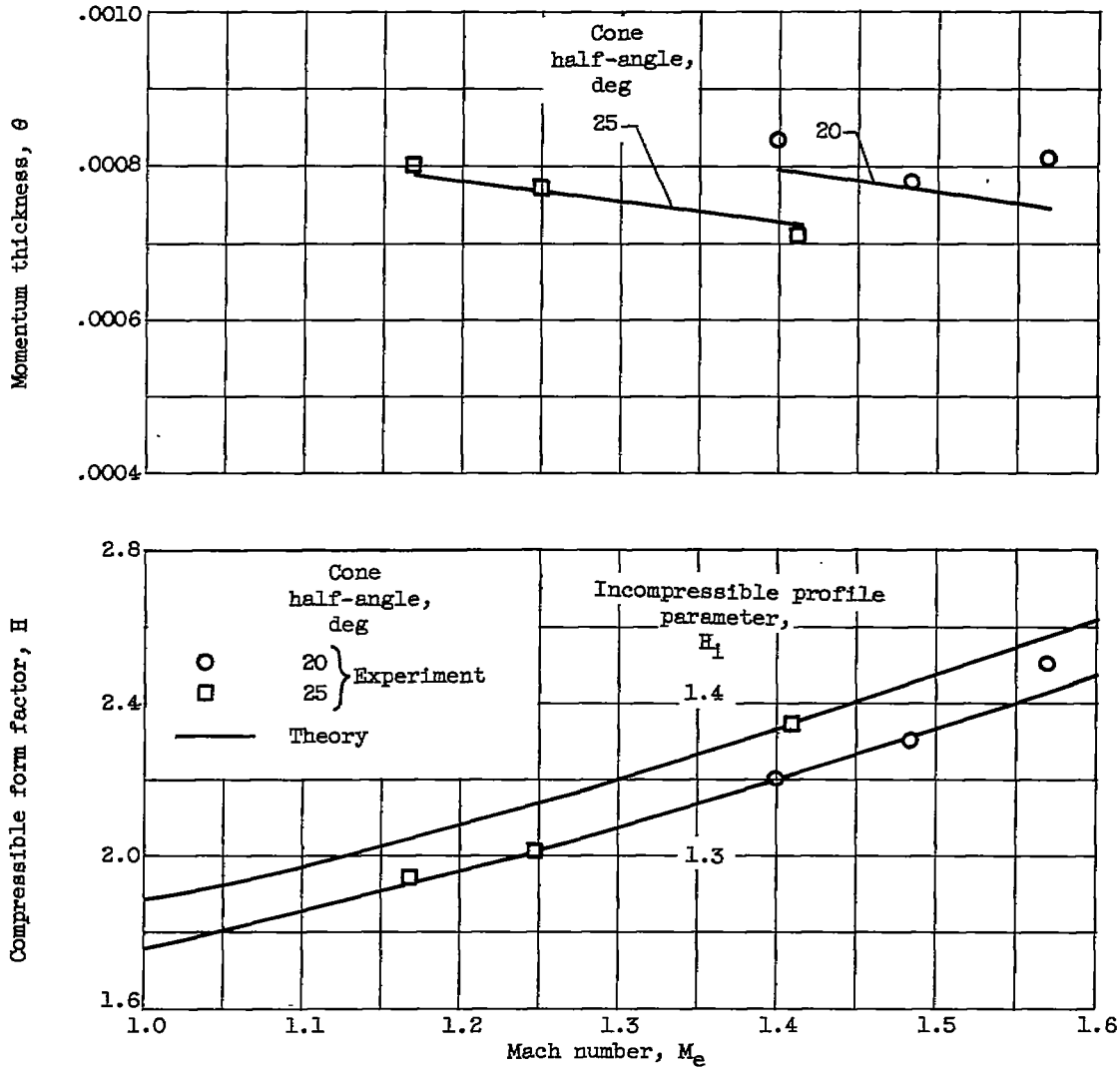

Figure 5. - Boundary layer on a cone (no pressure gradient).

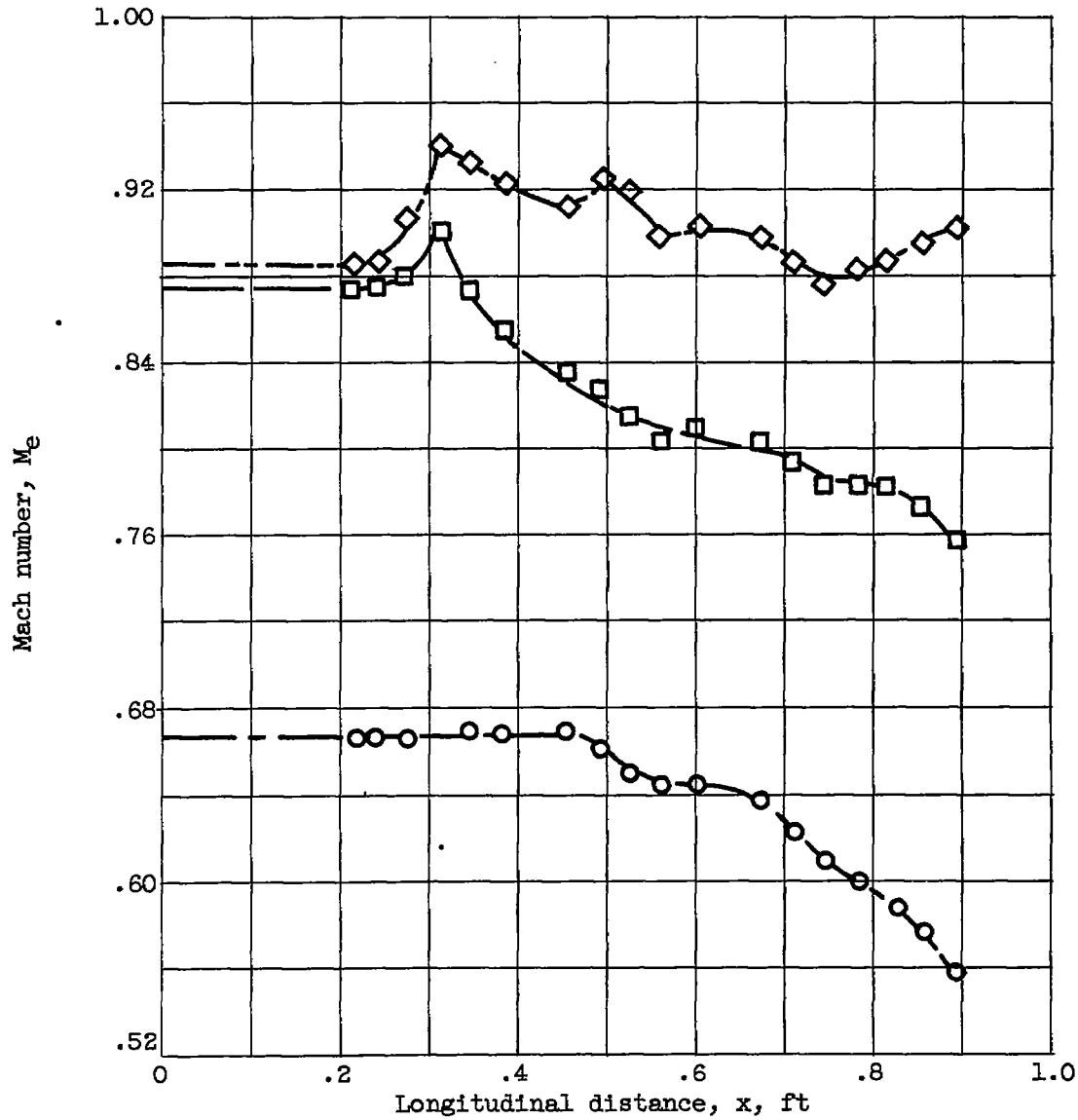

(a) Mach number gradient.

Figure 6. - Boundary layer on an axisymmetric body with moderate adverse pressure gradient.

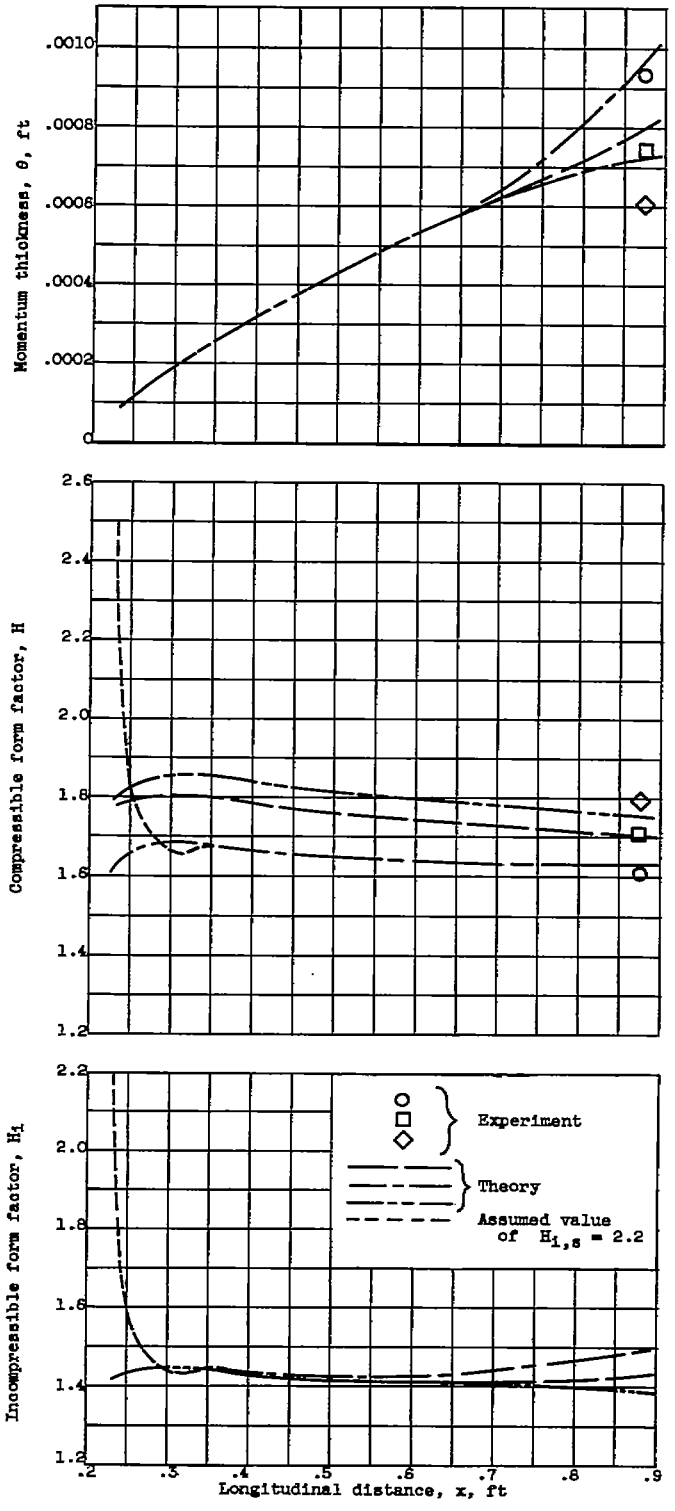

(b) Boundary-layer growth.

Figure 6. - Concluded. Boundary layer on an axisymmetric body with moderate adverse pressure gradient.

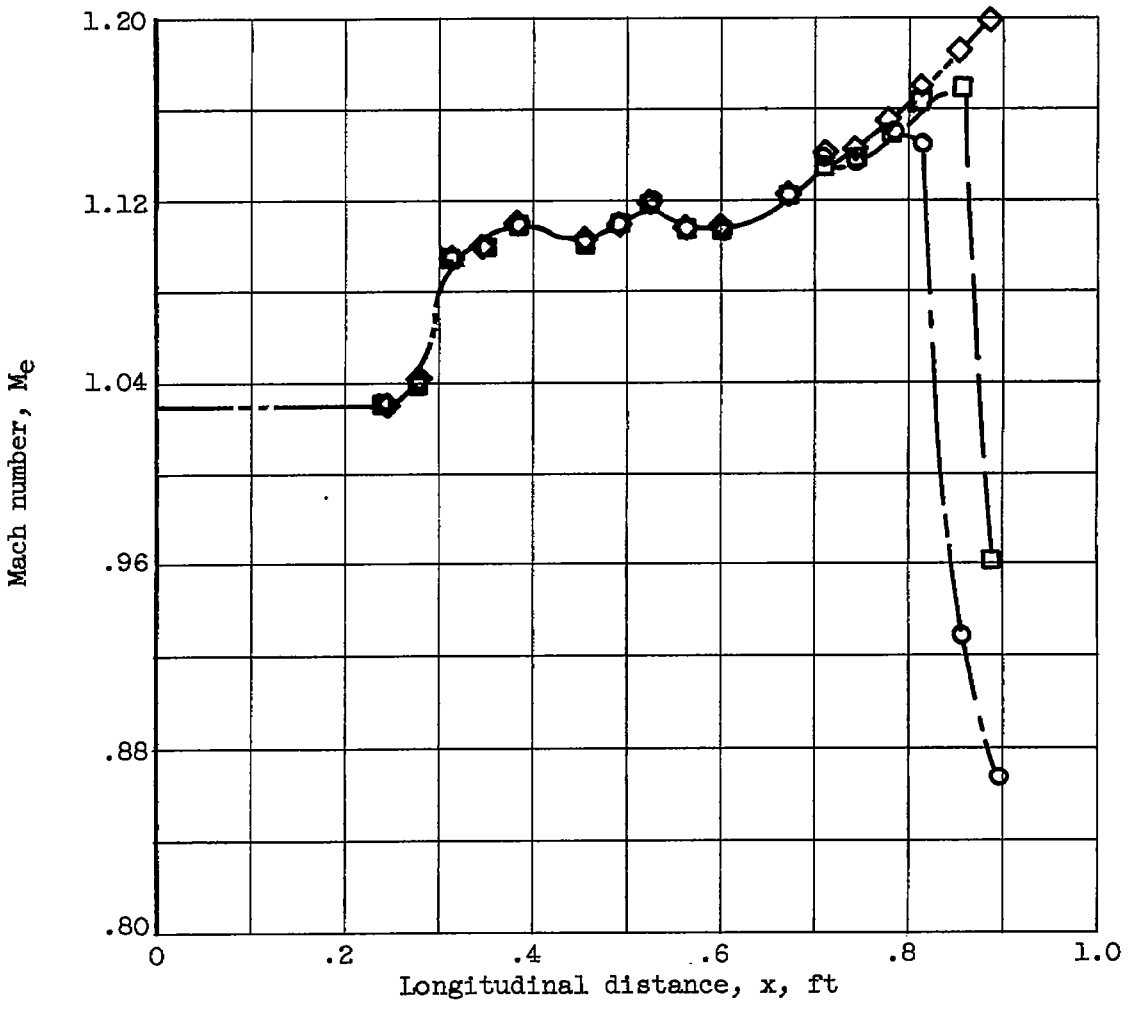

(a) Mach number gradient.

Figure 7. - Boundary layer on an axisymmetric body with high, adverse pressure gradient.

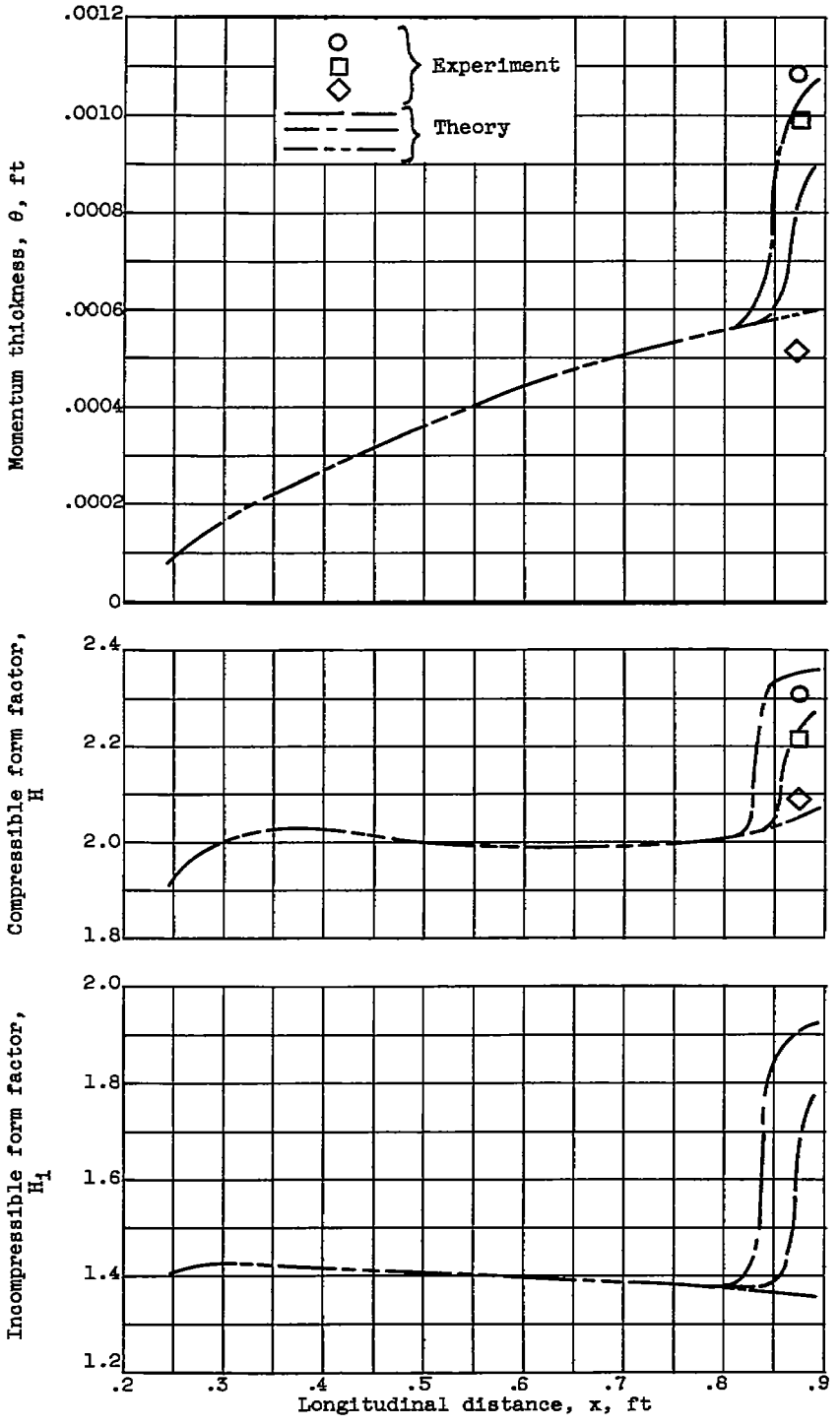

(b) Boundary-layer growth.

Figure 7. - Concluded. Boundary layer on an axisymmetric body with high, adverse pressure gradient.

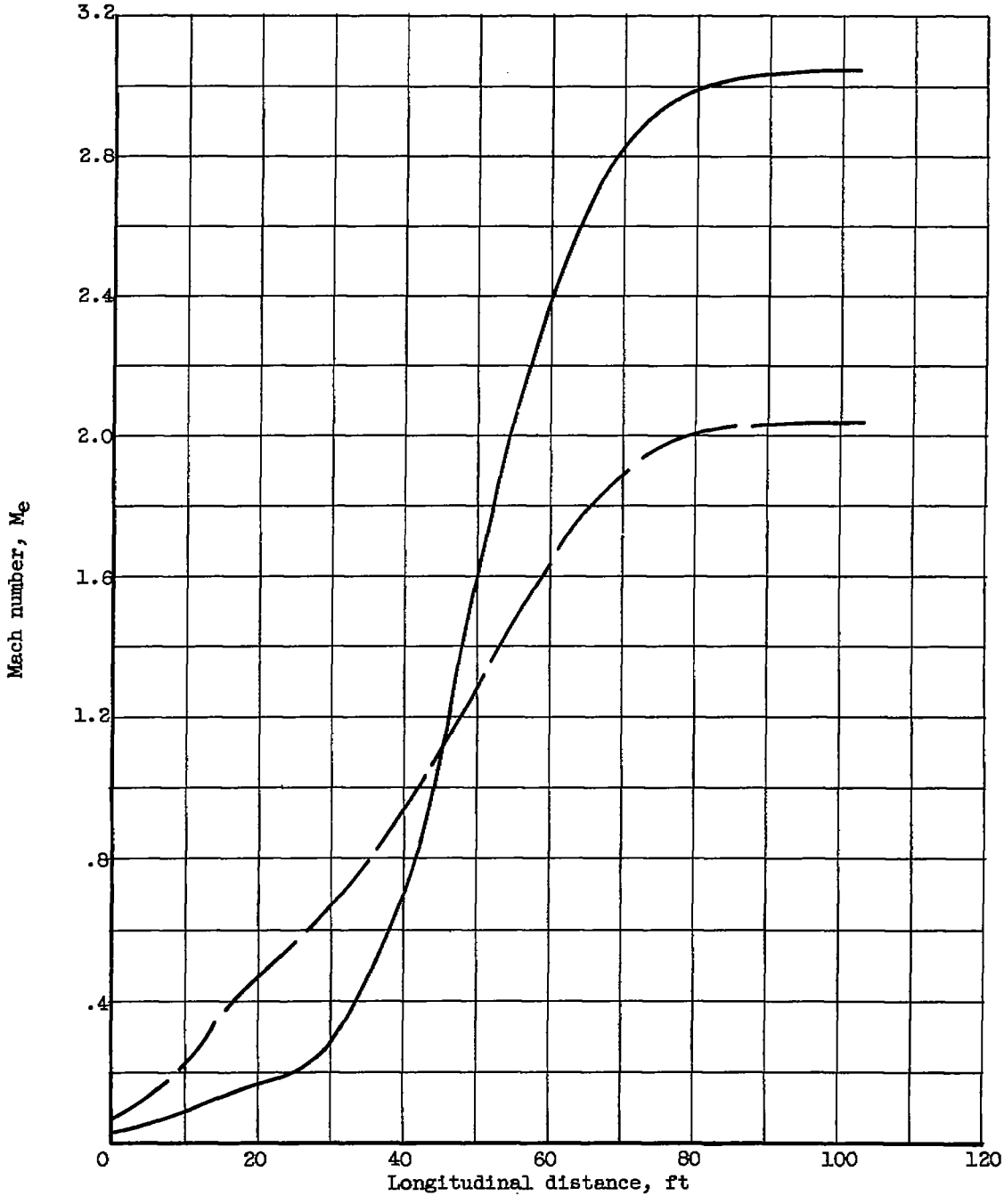

(a) Mach number gradient.

Figure 8. - Boundary layer on the walls of a wind tunnel with favorable pressure gradient.

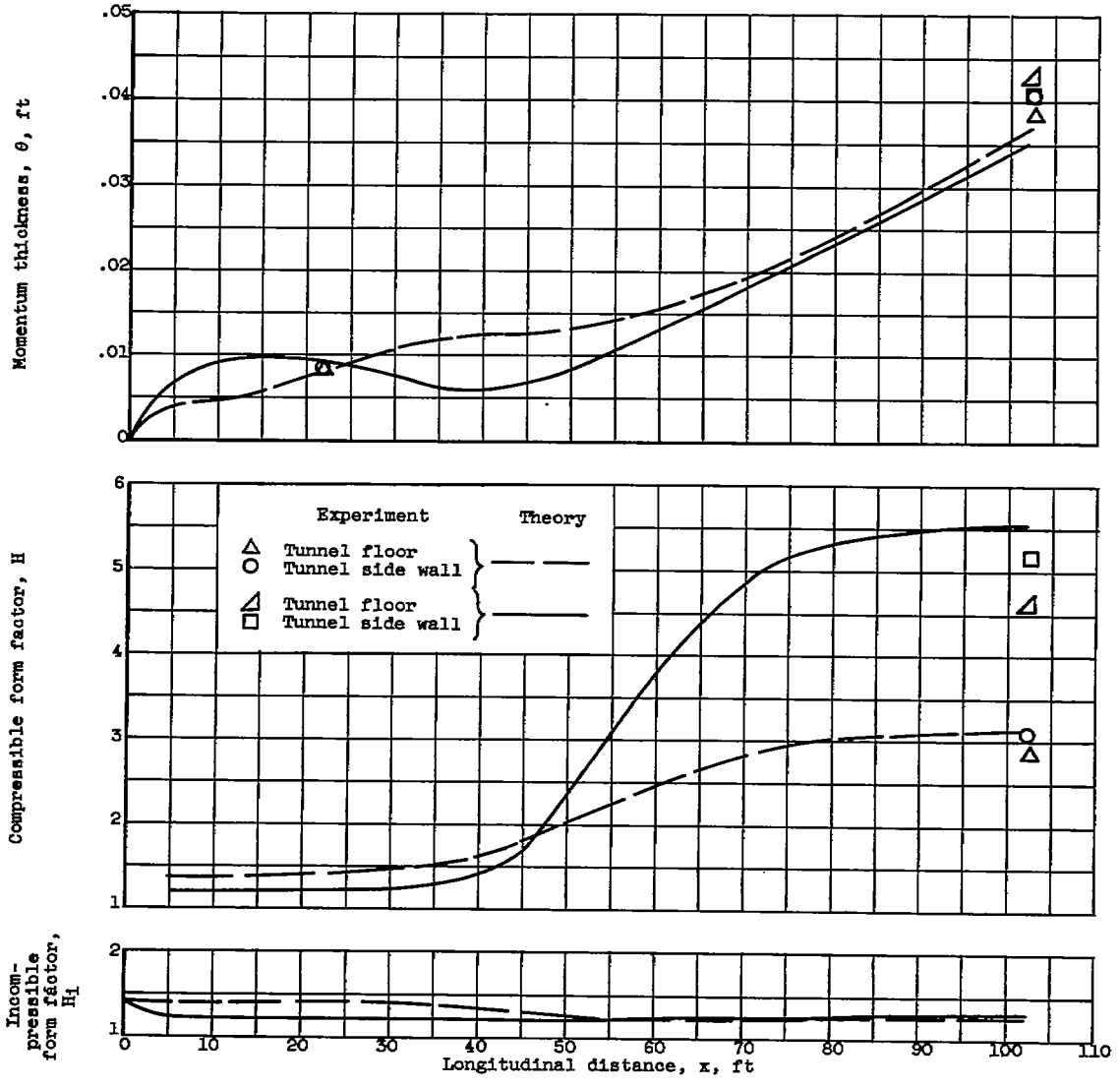

(b) Boundary-layer growth.

Figure 8. - Concluded. Boundary layer on the walls of a wind tunnel with favorable pressure gradient.